

Article

Compromised Vibration Isolator of Electric Power Generator Considering Self-Excitation and Basement Input

Young Whan Park, Tae-Wan Kim and Chan-Jung Kim * 

School of Mechanical Engineering, Pukyong National University, Busan 48513, Republic of Korea

* Correspondence: cjkim@pknu.ac.kr; Tel.: +82-51-629-6169

Abstract: A previous study proposed an optimal vibration isolator for self-excitation, but the solution results showed a critical drawback for the basement input. Because the plant system is exposed to self-excitation and basement input, the vibration isolator characteristics must meet all the requirements of both excitation cases. Two performance indices of the vibration isolator were introduced to evaluate the vibration control capability over two excitation cases, self-excitation and basement input, using the theoretical linear model of the electric power generator. The compromise strategy was devoted to enhancing the vibration control capability over the basement input, owing to the acceptable margin for self-excitation. The modification of the mechanical properties of the vibration isolator focused on the isolator between the mass block and the surrounding building. Simulation results revealed that an increase in the spring coefficient and a decrease in the damping coefficient of the vibration isolator beneath the mass block could enhance the vibration reduction capability over the basement input.

Keywords: vibration isolator; compromise strategy; theoretical linear model; performance index; electric power generator; basement input; self-excitation



Citation: Park, Y.W.; Kim, T.-W.; Kim, C.-J. Compromised Vibration Isolator of Electric Power Generator Considering Self-Excitation and Basement Input. *Inventions* **2023**, *8*, 40. <https://doi.org/10.3390/inventions8010040>

Academic Editor: Om P. Malik

Received: 15 December 2022

Revised: 19 January 2023

Accepted: 1 February 2023

Published: 2 February 2023



Copyright: © 2023 by the authors. Licensee MDPI, Basel, Switzerland. This article is an open access article distributed under the terms and conditions of the Creative Commons Attribution (CC BY) license (<https://creativecommons.org/licenses/by/4.0/>).

1. Introduction

A vibration isolator is necessary to control the vibration transmissibility between two connected systems. The mechanical property of the vibration isolator is the key design parameter for determining the vibration transfer from one system to another. The passive-type vibration isolator is widespread in industries owing to its low cost and simple installation. Therefore, passive-type vibration isolators are utilized in many applications to control the transmission of harsh excitations to protect supporting systems or preserve quiet environments [1–6]. The active-type mount device also performs well in many applications [7–10]. However, a proper control algorithm should be integrated into the mechanical–electronic system after rigorous identification of the supporting system [11–16]. In addition, the high cost of installation or maintenance is a critical hurdle for the increase in noise and vibration engineering market share.

The mechanism of the vibration isolator plays an essential role in fulfilling the objectives of vibration control over a complicated supporting system. Certain nonlinear factors may prevent the controllability of the supporting system, so novel mount design strategies are used to prevent technical problems [17–19]. A recent study proposed a simplified mount system that included a mass block adjacent to the vibration isolator and applied it to a power plant system [20]. The simplified vibration isolator was compared to the original multilayered isolator, including the mass block, using the measured response accelerations during full-payload operation. A response index was proposed and evaluated by varying the damping coefficient, and the feasibility of the proposed simple vibration isolator was discussed. However, the optimal condition of the vibration isolator was only effective for controlling the excitation from the power plant system and was ineffective for excitation generated from the basement location. The vibration isolator should be equally effective for both excitation cases, the power plant system, and the surrounding building.

This study selected an electric power generator that uses a combustion engine when an unusual power shortage occurs in a building as the target support system. The electric power generator was manufactured by the DAEHUNG Electric Machinery Company in South Korea, with a maximum capacity of up to 75 kW. The specific production was the same as described in a previous study [20]. Figure 1 shows the electric power generator.



Figure 1. Image of the electric power generator [20].

The combustion engine produces indispensable excitation during electric power generation at a constant rotational speed of 1800 rev/min. Six vibration isolators are used to support the electric power generator to prevent excitation transmission into the surrounding building, as shown in Figure 2.

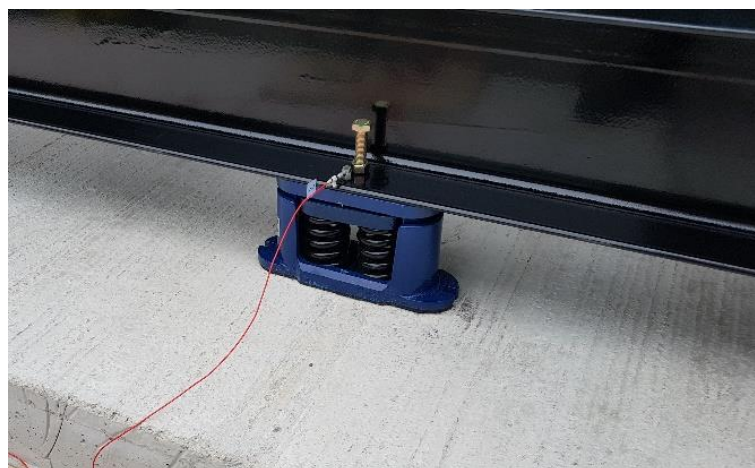


Figure 2. Image of vibration isolator [20].

The present vibration isolator showed reasonable efficiency in vibration control over self-excitation during operation, but the complex structure prevented quick maintenance service. To overcome this disadvantage, a previous study proposed a novel and simple mount structure without a mass block and compared it using the response index derived from the transmissibility formula for the basement response [20]. However, neither vibration isolator could evaluate any vibration-control capability under basement excitation. If an unexpected basement input is assigned, the supported electric power generator may fail to achieve structural stability owing to external perturbations from the basement. To

overcome these shortcomings of the original vibration isolator, a compromise strategy was applied in this study to select mechanical coefficients in the supporting isolators. This study established a theoretical linear model of the electric power generator to simulate the dynamic response or frequency response function (FRF) under several excitation conditions. Two performance indices were derived from the transmissibility between the two responses at different locations and under different excitation conditions. The first performance index represented the capability of the vibration isolator over self-excitation under operation between 30 Hz and 120 Hz, and the second index denoted the vibration control performance of the isolator over the basement input. The dynamic analysis of the electric power generator was focused on the modification of the mechanical properties, both the spring and damper coefficients, of the vibration isolator beneath the mass block. The compromise strategy was to reduce the second performance index while allowing an increase in the first performance index for a frequency range between 1 Hz and 120 Hz. However, because the proposed compromise strategy is only valid for the vibration isolator located at the bottom of the mass block, it may not be valid if the mechanism of the vibration isolators or supported plant system is changed.

2. Theoretical Linear Model of Supported Electric Power Generator

The capability of a vibration isolator can be identified from the dynamic response of the supporting system or attached basements. The performance of a supporting vibration isolator is possible with transmissibility between interesting responses using a theoretical model of an electric power generator. The supported electric power generator (M_p) is supported by a vibration isolator, which is attached to a mass block (M_M), as illustrated in Figure 3. The vibration isolator designed to support the power generator was modeled as linear mechanical elements, and both the stiffness coefficient K_p and damping coefficient C_p , and the connection between the mass block (M_M) and the surrounding building (M_B), were represented by the linear elements, the stiffness (K_M), and the damper (C_M). The responses of the three masses were defined as X_p , X_M , and X_B for the supporting power generator, mass block, and surrounding building, respectively, and X_B could be moved with the virtual spring coefficient (K_B) connected to the ground. The excitation forces from the supporting power plant and surrounding building were defined as F_p and F_B , respectively.

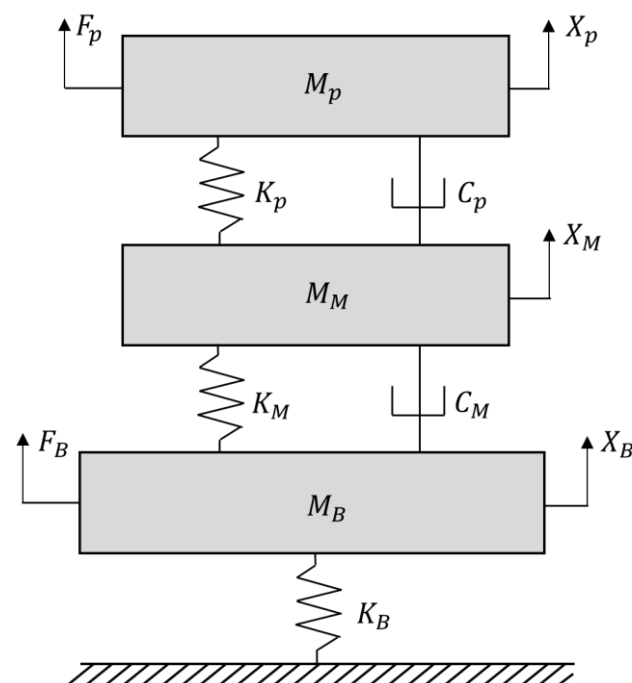


Figure 3. Equivalent electric power generator model supported by vibration isolators.

The dynamics of the supported power generator in Figure 3 can be simulated with theoretical modeling under the linear formulation of connection elements, coefficients of stiffness proportional to the displacement, and a viscous damping coefficient proportional to the velocity. All inertia terms, i.e., the power plant, mass block, and surrounding building, were assumed to be concentrated masses because the theoretical system model was focused on evaluating the vibration isolator alone. The governing equation for each concentrated mass is expressed as:

$$M_p \ddot{X}_p + C_p \dot{X}_p + K_p X_p = C_p \dot{X}_M + K_p X_M + F_p, \tag{1}$$

$$M_M \ddot{X}_M + (C_p + C_M) \dot{X}_M + (K_p + K_M) X_M = C_p \dot{X}_p + K_p X_p + C_M \dot{X}_B + K_M X_B, \tag{2}$$

$$M_B \ddot{X}_B + C_M \dot{X}_B + (K_M + K_B) X_B = C_M \dot{X}_M + K_M X_M + F_B \tag{3}$$

These equations can be expressed using the Laplace transformation in the s-domain to solve the responses under no initial values (both displacements and velocities), as shown in Equations (4)–(6).

$$\left[s^2 M_p + s C_p + K_p \right] X_p(s) = \left[s C_p + K_p \right] X_M(s) + F_p(s), \tag{4}$$

$$\begin{aligned} \left[s^2 M_M + s(C_p + C_M) + (K_p + K_M) \right] X_M(s) \\ = \left[s C_p + K_p \right] X_p(s) + \left[s C_p + K_p \right] X_M(s), \end{aligned} \tag{5}$$

$$\left[s^2 M_B + s C_M + (K_M + K_B) \right] X_B(s) = s C_M X_M(s) + K_M X_M + F_B(s) \tag{6}$$

The governing equations can be simplified using the three temporary terms in Equations (7a)–(7c), and the FRF of the supporting power generator can be derived from Equation (8) over the power plant input F_p ($F_B = 0$) and surrounding building response X_B . In addition, the FRF between the excitation F_B and the response at the power plant X_B can be derived, as shown in Equation (9).

$$\alpha(s) = s^2 M_p + s C_p + K_p, \tag{7a}$$

$$\beta(s) = s^2 M_M + s(C_p + C_M) + (K_p + K_M), \tag{7b}$$

$$\gamma(s) = s^2 M_B + s C_M + (K_M + K_B), \tag{7c}$$

$$\frac{X_B(s)}{F_p(s)} = H_{X_B} = \frac{(s C_M + K_M)(s C_p + K_p)}{\alpha(s)\beta(s)\gamma(s) - \alpha(s)(s C_M + K_M)^2 - \gamma(s)(s C_p + K_p)^2}, \tag{8}$$

$$\frac{X_p(s)}{F_p(s)} = H_{X_p} = \frac{\beta(s)\gamma(s) - (s C_M + K_M)^2}{\alpha(s)\beta(s)\gamma(s) - \alpha(s)(s C_M + K_M)^2 - \gamma(s)(s C_p + K_p)^2} \tag{9}$$

3. Evaluation Indices for Vibration Isolator

If the electric power generator is operated under the rated operational condition, self-excitation can be represented by F_p under no basement force ($F_M = 0$). Two vibration isolators can passively control self-excitation and the transmissibility between X_B and X_p can be formulated into the first performance index (I_1) using Equations (8) and (9). Here, I_1 denotes the vibration transmissibility from the power plant to the surrounding building. This means that the first performance index in Equation (10) represents the vibration isolator’s capability to control the power generator’s excitation. The smaller the first index value, the better the self-excitation performance of the vibration isolator.

$$I_1(s) = \frac{X_B(s)}{X_p(s)} = \frac{H_{X_B}}{H_{X_p}} = \frac{(s C_M + K_M)(s C_p + K_p)}{\beta(s)\gamma(s) - (s C_M + K_M)^2} \tag{10}$$

The performance of the vibration isolator over the basement input can be derived for the no external force condition ($F_M = F_p = 0$) because the basement input was assigned as the displacement or velocity of basements [21,22]. Under the no external force condition, the ratio between X_p and X_M can be derived using Equations (4) and (6), as shown in Equation (11). The second performance index (I_2) represents the vibration reduction capability of the vibration isolator under basement input conditions. The smaller the second index value, the better the vibration isolator performance for the basement input.

$$I_2(s) = \frac{X_p(s)}{X_B(s)} = \frac{\gamma(s)(sC_p + K_p)}{\alpha(s)(sC_M + K_M)} \tag{11}$$

4. Dynamic Simulation of Supported Power Plant Model

The simulation model of the power generator was studied for the same specifications considered in a previous study [20]. The theoretical model of the power generator is used for the linear formula in Figure 3, and the mechanical properties of the vibration isolator, C_p and K_p , were obtained experimentally using a test machine (835 model/MTS systems, Eden Prairie, Minnesota, United States). Other linear connecting elements were tuned using the response accelerations during full-load operation of the min constant 1800 rev/ internal combustion engine. The parameters defined in Table 1 are verified based on experimental data from a previous study [20].

Table 1. Specification of theoretical power plant model [20].

Variable	Value
M_p (kg)	6070
M_M (kg)	6900
M_B (kg)	$10 \times M_p$
K_p (kN/m)	940 (1 Hz), 1050 (30 Hz), 1245 (60 Hz), 1881 (90 Hz), 4399 (120 Hz)
K_M (kN/m)	$(5 \times 10^6) \times K_p$
K_B (kN/m)	$10^{-1} \times K_p$
C_p (Nsec/m)	603 (1 Hz), 376 (30 Hz), 216 (60 Hz), 184 (90 Hz), 158 (120 Hz)
C_M (Nsec/m)	$(1.5 \times 10^6) * C_p$

The dynamics of the theoretical power plant model can be evaluated via the FRFs formulated using Equations (8) and (9). The frequency of interest was set between 1 Hz and 120 Hz under the operational speed of the combustion engine, and the simulation result is plotted in Figure 4.

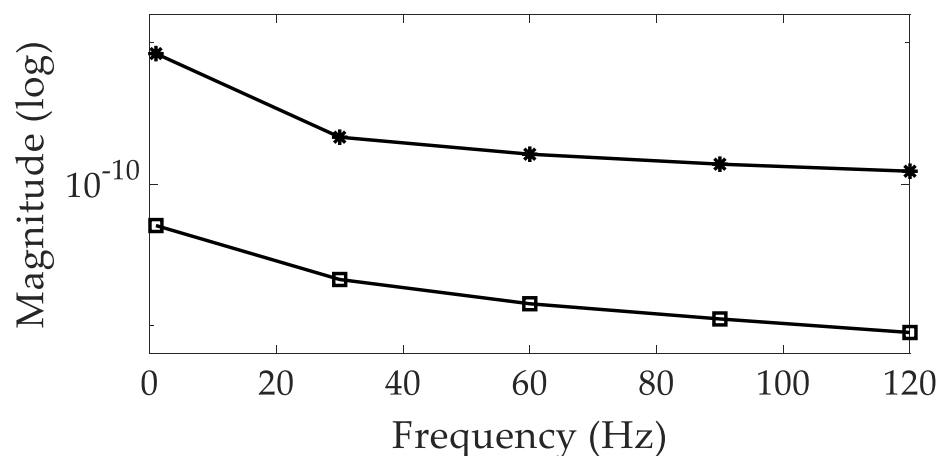


Figure 4. FRF of the theoretical power plant model. \square : H_{X_p} , \times : H_{X_B} .

The FRFs showed that the supported electric power generator model had no resonance frequencies for the frequency range of interest, so the original mechanical coefficients of the vibration isolator, C_p , K_p , C_M , and K_M , were suitably selected. The performance of the vibration isolator is also evaluated using the first and second performance indices, plotted in Figures 5 and 6, respectively. Both indices indicated that the transmissibility from the power plant to the surrounding building was very small. In contrast, the transmissibility from the mass block to the power plant was relatively high for the frequency range of interest. Therefore, the controllability of the vibration isolator was reliable when excitation was induced from the supporting power plant side. However, the capability of the vibration isolator to control the excitation from the basement side is not acceptable under the original mechanical property conditions (see Table 1).

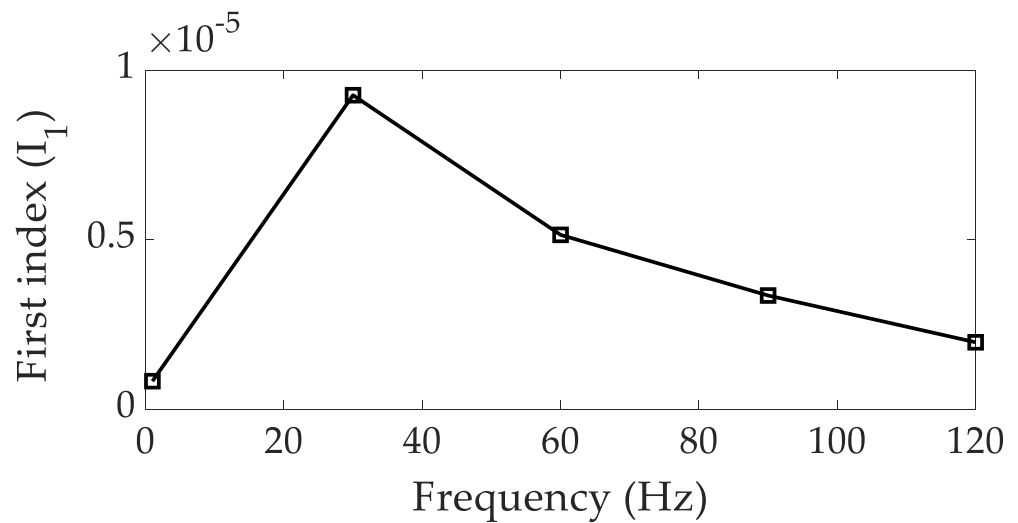


Figure 5. Variation in the first performance index as a function of frequency.

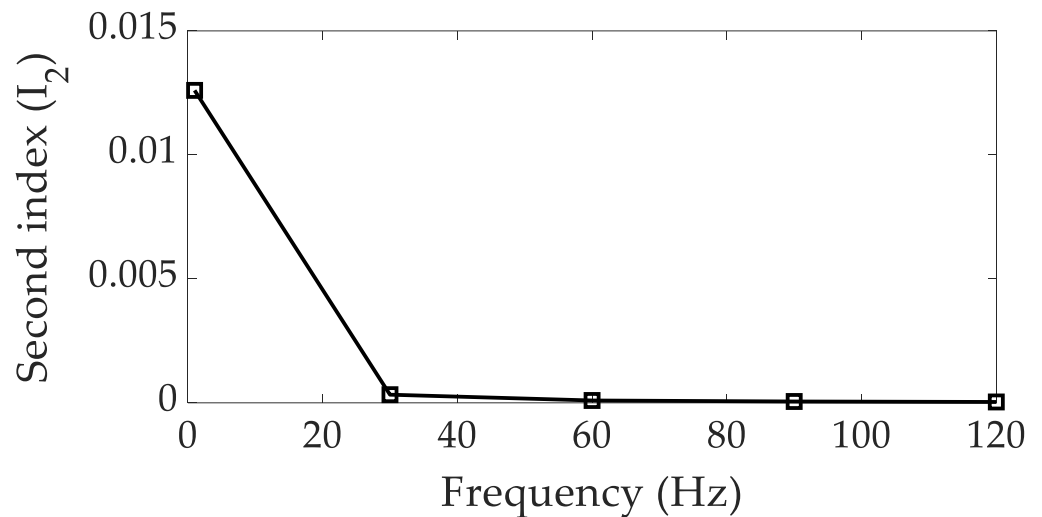


Figure 6. Variation in the second performance index as a function of frequency.

To overcome the poor capability of vibration control over the vibration input from the mass block, revised mechanical properties of the vibration isolator were required for the power plant model. In particular, the mechanical properties of the two vibration isolators cannot be arbitrarily modified from a physical point of view because it is challenging to achieve most mechanical coefficients using isolator specimens, springs, or dampers. Therefore, the modification of coefficients in the vibration isolator should be increased or decreased in proportion to the measured dynamic stiffness and damping coefficient.

Between the two vibration isolators, the vibration isolator beneath the mass block (C_M, K_M) was selected to evaluate the two performance indices in different modification coefficient situations. The vibration isolator (C_p, K_p) to the electric power generator was not considered because the effect of the mass block and the related adjacent joint was considered in a previous study [20] and owing to the high cost of installation or maintenance of the electric power generator. Four vibration isolator cases are selected from the original values, as summarized in Table 2.

Table 2. Modified mechanical properties of vibration isolator.

Case	Value
I	$C_M \div 10, K_M \div 10$
II	$C_M \div 10, K_M \times 10$
III	$C_M \times 10, K_M \div 10$
IV	$C_M \times 10, K_M \times 10$

Two indices of the theoretical power generator model were calculated for the selected frequency range in all four cases. The variation in each performance index was calculated as the ratio of the modified index to the original value. The detailed calculation results are summarized in Tables 3 and 4.

Table 3. Ratio of the first performance index for four vibration isolator cases.

Case	Ratio of the First Performance Index (I_1)				
	1 (Hz)	30 (Hz)	60 (Hz)	90 (Hz)	120 (Hz)
I	-	3.2	1.6	1.4	1.6
II	-	3.2	1.7	1.5	1.6
III	-	3.2	1.6	1.4	1.6
IV	-	3.2	1.6	1.4	1.6

Table 4. Ratio of the second performance index for four vibration isolator cases.

Case	Ratio of the Second Performance Index (I_2)				
	1 (Hz)	30 (Hz)	60 (Hz)	90 (Hz)	120 (Hz)
I	1.3	1.0	1.2	1.5	2.0
II	1.3	0.9	0.9	0.8	0.8
III	1.3	1.0	1.0	1.0	1.0
IV	1.3	1.0	1.0	1.0	1.0

The two performance indices exhibited different values in the frequency range of interest by varying the element coefficients. Because the two ratios of performance indicators show the amount of change compared to the reference vibration isolator condition, it can be concluded that the smaller the value, the better the vibration isolator performance under the applied stiffness or damping coefficients. Conversely, when the ratio of index value is greater than 1, it can be determined that the vibration isolator performance is degraded compared to the reference condition. The index ratio at 1 Hz was not considered because self-excitation from the electric power generator was observed only between 30 Hz and 120 Hz. The optimal result is Case II, where the damping coefficient decreases and the stiffness coefficient increases. The other three cases showed similar results for the two performance indices; therefore, the combination of an increase and a decrease in the mechanical coefficients is essential for vibration control from the vibration isolators.

5. Compromise Strategy of Vibration Isolator

The selected target power generator has been reported to have more than ten times the margin at the basement response under full-load operation [20]. However, the capability of vibration control over the basement input was not guaranteed at all. The objective vibration isolator was preliminarily selected for the isolator (C_M, K_M) located beneath the mass block, and the upper vibration isolator (C_p, K_p) was not changed. The simulation results revealed that the best condition for the vibration isolator was an increase in the spring coefficient and a decrease in the damping coefficient. For a ten-fold increase in the spring coefficient and a ten-fold decrease in the damping coefficient, the second performance index was reduced by up to 20% in the high-frequency range; the first performance index was increased up to 320% at 30 Hz. Because the first performance index has a large margin of more than ten times that of the original vibration isolator equipment, the second performance index can be effectively decreased by following the modification guideline with an increase in the stiffness coefficient as well as a decrease in the damping coefficient at the lower vibration isolator. Therefore, it can enhance the vibration control capability of the vibration isolator over a basement input, while decreasing the vibration control performance for self-excitation of the electric power generator.

However, this compromise strategy has some drawbacks. First, the second performance index increased at 1 Hz, which may coincide with the critical frequency for earthquake events. Second, the theoretical linear model was not validated for a low-frequency range of less than 30 Hz. Third, the experiments did not fully verify the feasibility of the design modification of the vibration isolator for Case II. Additional performance enhancement is possible with the modification of the upper vibration isolator (C_p, K_p) in future work.

6. Conclusions

The compromise strategy regarding the vibration isolator for an electric power generator was investigated via simulation of a theoretical linear model. Two vibration isolators (upper and lower) were modeled as linear connecting elements—the spring and damping coefficients. The supporting targets were simplified as concentrated masses. All mechanical specifications followed the system parameters verified in a previous study, and four cases of coefficient modifications were selected for the lower vibration isolator (C_M, K_M). The simulation results revealed that the best case was derived for the combination of isolator coefficients that increases the stiffness coefficient and decreases the damping coefficient, which is expected to decrease the second performance index by 20%. In the same case, the first performance index was increased to 320% at 30 (Hz), so a compromise strategy should be applied to this situation. A previous study verified that the acceptable response margin could be expected to be up to ten times that of the original equipment. Therefore, conditions in Case II were found to be appropriate for the electric power generator.

Author Contributions: Conceptualization, formal analysis, Y.W.P.; software, investigation, T.-W.K.; validation, writing—original draft, visualization, C.-J.K. All authors have read and agreed to the published version of the manuscript.

Funding: This research was supported by the Pukyong National University Development Project Research Fund, 2022.

Data Availability Statement: The data presented in this study are available on request from the corresponding author.

Acknowledgments: This research was supported by Pukyong National University.

Conflicts of Interest: The authors declare no conflict of interest.

References

1. Alujevic, N.; Cakmak, D.; Wolf, H.; Jokic, M. Passive and active vibration isolation system using inerter. *J. Sound Vib.* **2018**, *418*, 163–183. [[CrossRef](#)]
2. Siami, A.; Karimi, H.R.; Cigada, A.; Zappa, E.; Sabbioni, E. Parameter optimization of an inerter-based isolator for passive vibration control of Michelangelo's Rondanini Pieta. *Mech. Syst. Signal Process.* **2018**, *98*, 667–683. [[CrossRef](#)]
3. Wu, Z.; Jing, X.; Sun, B.; Li, F. A 6DOF passive vibration isolator using X-shape supporting structures. *J. Sound Vib.* **2016**, *380*, 90–111. [[CrossRef](#)]
4. Lee, J.; Okwudire, C.E. Reduction of vibrations of passively-isolated ultra-precision manufacturing machines using mode coupling. *Precis. Eng.* **2016**, *43*, 164–177. [[CrossRef](#)]
5. Ribeiro, E.A.; Lopes, E.M.O.; Bavastri, C.A. A numerical and experimental study on optimal design of multi-DOF viscoelastic supports for passive vibration control in rotating machinery. *J. Sound Vib.* **2017**, *411*, 346–361. [[CrossRef](#)]
6. Oh, H.U.; Lee, K.J.; Jo, M.S. A passive launch and on-orbit vibration isolation system for the spaceborne cryocooler. *Aerosp. Sci. Technol.* **2013**, *28*, 324–331. [[CrossRef](#)]
7. Gu, X.; Yu, Y.; Li, J.; Li, Y. Semi-active control of magnetorheological elastomer base isolation system utilizing learning-based inverse model. *J. Sound Vib.* **2017**, *406*, 346–362. [[CrossRef](#)]
8. Santos, M.B.; Coelho, H.T.; Neto, F.P.L.; Mafhoud, J. Assessment of semi-active friction dampers. *Mech. Syst. Signal Process.* **2017**, *94*, 33–56. [[CrossRef](#)]
9. Oh, H.U.; Choi, Y.J. Enhancement of pointing performance by semi-active variable damping isolator with strategies for attenuating chattering effects. *Sens. Actuators A Phys.* **2011**, *165*, 385–391. [[CrossRef](#)]
10. Azadi, M.; Behzadipour, S.; Faulkner, G. Performance analysis of a semi-active mount made by a new variable stiffness spring. *J. Sound Vib.* **2011**, *330*, 2733–2746. [[CrossRef](#)]
11. Pingzhang, Z.; Jianbin, D.; Zhenhua, L. Simultaneous topology optimization of supporting structure and loci of isolators in an active vibration isolation system. *Comput. Struct.* **2018**, *194*, 74–85.
12. Beijen, M.A.; Tjepkema, D.; Dijk, J. Two-sensor control in active vibration isolation using hard mounts. *Control Eng. Pract.* **2014**, *26*, 82–90. [[CrossRef](#)]
13. Yang, X.L.; Wu, H.T.; Li, Y.; Chen, B. Dynamic isotropic design and decentralized active control of a six-axis vibration isolator via Stewart platform. *Mech. Mach. Theory* **2017**, *117*, 244–252. [[CrossRef](#)]
14. Wang, Z.; Mak, C.M. Application of a movable active vibration control system on a floating raft. *J. Sound Vib.* **2018**, *414*, 233–244. [[CrossRef](#)]
15. Li, Y.; He, L.; Shuai, C.G.; Wang, C.Y. Improved hybrid isolator with maglev actuator integrated in air spring for active-passive isolation of ship machinery vibration. *J. Sound Vib.* **2017**, *407*, 226–239. [[CrossRef](#)]
16. Chi, W.; Cao, D.; Wang, D.; Tang, J.; Nie, Y.; Huang, W. Design and experimental study of a VCM-based stewart parallel mechanism used for active vibration isolation. *Energies* **2015**, *8*, 8001–8019. [[CrossRef](#)]
17. Yang, J.; Xiong, Y.P.; Xing, J.T. Vibration power flow and force transmission behavior of a nonlinear isolator mounted on a nonlinear base. *Int. J. Mech. Sci.* **2016**, *115*, 238–252. [[CrossRef](#)]
18. Hu, Z.; Zheng, G. A combined dynamic analysis method for geometrically nonlinear vibration isolation with elastic rings. *Mech. Syst. Signal Process.* **2016**, *76*, 634–648. [[CrossRef](#)]
19. Yan, L.; Gong, X. Experimental study of vibration isolation characteristics of a geometric anti-spring isolator. *Appl. Sci.* **2017**, *7*, 711. [[CrossRef](#)]
20. Kim, C.-J. Design criterion of damper component of passive-type mount module without using base mass-block. *Energies* **2018**, *11*, 1548. [[CrossRef](#)]
21. Rao, S.S. *Mechanical Vibration*, 5th ed.; Pearson: Singapore, 2011.
22. Inman, D.J. *Engineering Vibration*, 4th ed.; Pearson: Singapore, 2013.

Disclaimer/Publisher's Note: The statements, opinions and data contained in all publications are solely those of the individual author(s) and contributor(s) and not of MDPI and/or the editor(s). MDPI and/or the editor(s) disclaim responsibility for any injury to people or property resulting from any ideas, methods, instructions or products referred to in the content.